International Journal of Biological Macromolecules 124 (2019) 444–450

Contents lists available at ScienceDirect

International Journal of Biological Macromolecules

journal homepage: http://www.elsevier.com/locate/ijbiomac

Cell behavior on the alginate-coated PLLA/PLGA scaffolds

Gokhan Bahcecioglu [a,b,c], Nesrin Hasirci [a,c,d], Vasif Hasirci [a,b,c,e,*]

[a] BIOMATEN, Middle East Technical University (METU) Center of Excellence in Biomaterials and Tissue Engineering, Ankara, Turkey
[b] Department of Biological Sciences, METU, Ankara, Turkey
[c] Graduate Department of Biotechnology, METU, Ankara, Turkey
[d] Department of Chemistry, METU, Ankara, Turkey
[e] Department of Medical Engineering, Acibadem Mehmet Ali Aydinlar University, Atasehir, Istanbul, Turkey

ARTICLE INFO

Article history:
Received 10 September 2018
Received in revised form 27 October 2018
Accepted 17 November 2018
Available online 19 November 2018

ABSTRACT

Here, we investigated the effect of preparation temperature and alginate-coating on L929 fibroblast behavior on lyophilized microporous PLLA/PLGA (95:5, w/w) scaffolds. The lower freezing temperature used during lyophilization (−80 °C) resulted in smaller pores (around 50 μm) and higher compressive modulus (1500 kPa) than those prepared at the higher temperature (−20 °C) (pore size: 120 μm, compressive modulus: 600 kPa) ($p < 0.01$). Cell proliferation was significantly lower on the alginate-coated scaffolds ($p < 0.05$), probably due to weak cell adhesion on alginate, rapid degradation/dissolution of the alginate hydrogel (40% weight loss after 2 weeks of incubation) ($p < 0.05$), which resulted in loss of material and cells, and the decrease in the pH ($p < 0.05$), which probably resulted in decreased cell metabolic activity. Cells tended to get less round on the scaffolds prepared at −20 °C, which had lower compressive modulus and larger pores, and upon coating with alginate, which resulted in a hydrophilic surface that had lower stiffness. When the scaffolds had closer stiffness to the cells, the cells tended to get more branched. The most branched morphology of the fibroblasts was obtained in the presence of alginate, a natural polymer having a similar stiffness with that of the L929 fibroblasts (4 kPa).

1. Introduction

Tissue engineering aims at restoring, maintaining or replacing the biological functions of an injured tissue by using cells, scaffolds, and bioactive molecules [1]. Cells produce extracellular matrix (ECM) which leads to new tissue formation. Bioactive molecules such as growth factors help in regulating cell functions, including cell migration, proliferation, differentiation or ECM deposition [2,3]. Scaffolds, on the other hand, support and guide the cells to produce the new tissue [4,5]. It is desirable that the scaffold degrades at a controllable rate that matches the regeneration rate of the target tissue without causing any adverse effect in the body, and the space left behind is filled with the newly formed tissue [6]. An ideal scaffold should be porous so as to provide space for the cells to migrate and produce the new tissue, and to transport the nutrients, oxygen, and waste products [7]. When implanted in the body, it should provide the mechanical strength to withstand the stress applied on it until it is degraded [8].

The cell's response to a scaffold is the main indicator of appropriateness of that scaffold for the cell to grow and produce a functional target tissue, because cell behavior mainly depends on the balance between cell-cell and cell-matrix interactions [9,10]. The main parameters that regulate cell behavior are scaffold microarchitecture (porosity and pore size), mechanical properties (stiffness, hardness and modulus), and surface chemistry (hydrophilicity, presence of functional groups). For instance, porosity contributes not only to nutrient permeability, but also to cell spreading and migration [11–13]. Appropriate pore size and interconnectivity are important for cell spreading and tissue ingrowth as well as permeability [12–21]. Mechanical properties of the scaffolds play a major role in cell adhesion, spreading and migration [22–35]. Similarly, surface chemistry also directs cell adhesion and spreading [36–39].

In the literature, there have been a wide range of research on the effects of scaffold properties on cell morphology, which is the main indicator of cell-material interactions [23,24,27,29–34]. However, these studies report controversial results; some have shown increased cell spreading when the scaffold gets stiffer [23,27,30,31], while others have shown decreased spreading [29,32–34]. Ni and colleagues [40] have predicted in their theoretical model that a cell would get a more branched morphology when the stiffness of the scaffold it resides on gets closer to the stiffness of the cell itself. Recently, we have experimentally shown that each cell type exhibits a different behavior on the scaffolds depending on the modulus of the cell itself and the strut modulus of the scaffold [5]. We have tested the spreading behavior of L929 fibroblasts and human meniscal fibrochondrocytes on 3D

* Corresponding author at: BIOMATEN, METU Center of Excellence in Biomaterials and Tissue Engineering, Dumlupinar Blvd No: 1, Cankaya, Ankara 06800, Turkey.
E-mail address: vhasirci@metu.edu.tr (V. Hasirci).

https://doi.org/10.1016/j.ijbiomac.2018.11.169
0141-8130/

microporous poly(L-lactic acid) (PLLA)/poly(lactic acid-*co*-glycolic acid) (PLGA) scaffolds and shown that fibroblasts which are soft (stiffness: around 4 kPa) [41] tend to assume a more round morphology on the scaffolds with the increasing strut modulus, while fibrochondrocytes which are stiffer (stiffness: 28–150 kPa) [42] tend to exhibit a more elongated behavior. In fact, morphology of the cells in the native tissues may also vary depending on their location in the tissue which may have different stiffness values. For example, fibrochondrocytes in the outer region of the meniscus, which is stiffer, are more elongated or dendritic, while those in the inner region, which is softer, are more round or polygonal [42]. Similarly, although conventionally considered as spindle-shaped cells, fibroblasts assume spindle-shaped morphology in the superficial papillary layer of the dermis and round or polygonal morphology in deeper reticular layer [43]. These studies show that the morphology and phenotype of a cell could be directed to assume different morphologies and phenotypes, by changing the scaffold properties such as microarchitecture, surface stiffness and hydrophilicity.

In the current study, microporous PLLA/PLGA scaffolds of different bulk stiffness were produced by lyophilization and coated with alginate, a natural hydrophilic polymer that forms a soft hydrogel upon crosslinking with calcium ions (modulus: around 4 kPa) [44]. The scaffolds were seeded with L929 mouse fibroblasts, one of the most frequently used cells in evaluation of cell behavior and/or cytotoxicity [25,45], and incubated for 2 weeks. The effects of microarchitecture, stiffness and alginate-coating on the proliferation and morphology of cells were examined.

2. Materials and methods

2.1. Materials

Poly(L-lactic acid) (PLLA) with a viscosity of 3.2–3.8 dL/g (Mv: 150 kDa) was purchased from FORUSORB (China). Poly(L-lactic acid-*co*-glycolic acid) (PLGA, 50:50) (Mv: 46 kDa) was purchased from Boehringer Ingelheim (Germany). Calcium chloride and 1,4-dioxane were from Merck (Germany). Sodium alginate (low viscosity), penicillin-streptomycin, and fetal bovine serum (FBS) were from Sigma (USA). Dulbecco's modified Eagle's medium (DMEM-High glucose), Alexa fluor 532-phalloidin, DRAQ5 were from Thermo Fisher Scientific (USA).

2.2. Methods

2.2.1. Preparation of the scaffolds

PLLA/PLGA (95:5, w/w) solution (3%, w/v in 1,4-dioxane) was prepared in a glass Petri dish, frozen at −20 °C or −80 °C, and lyophilized for 10 h. Scaffolds were cut into cubes of $5 \times 5 \times 5$ mm^3, exposed to oxygen plasma (100 W, 20 mTorr) for 1 min, and soaked in sodium alginate solution (1%, w/v), washed and then soaked in calcium chloride solution (5%, w/v) to crosslink the alginate (Coated scaffolds, C). Some of the scaffolds were oxygen plasma-treated, but not coated with alginate (Uncoated scaffolds, UC).

2.2.2. Scanning electron microscopy

The scaffolds were sectioned, and sputter-coated with gold-palladium, and analyzed using a scanning electron microscope (SEM) (FEI, Quanta 200F, USA) under high vacuum. SEM images ($n = 5$ images/sample) of the scaffolds ($n = 2$ samples) were analyzed using the ImageJ software (NIH), to determine the porosity and pore size of the scaffolds.

2.2.3. Mercury porosimetry

Pore size distribution was determined using a mercury porosimeter Poremaster 60 (Quantachrome Corporation, USA). The tests were performed under 0–50 psi pressure, 140° contact angle, and 480 dyne/cm surface tension.

2.2.4. Mechanical testing

Compression tests were done using a mechanical tester (Stable Micro Systems, MT-LQ, UK), with a 100 N cell load, at a displacement rate of 10 mm/min. Compressive modulus and compressive strength of the scaffolds in wet state (after incubation for 24 h in 0.01 M phosphate buffer saline (PBS, pH 7.2)) were calculated from the elastic region of the stress-strain curve as described previously [46].

2.2.5. Degradation of the scaffolds

For degradation tests, scaffolds ($n = 3$) were incubated for 8 weeks in centrifuge tubes containing 0.01 M PBS (pH 7.2) and placed on a shaker operating at 50 rpm, 37 °C. At each time point (Weeks 2, 4, 6, and 8), the samples were removed from PBS, vacuum dried (70 °C, 5 h), and weighed on an analytical balance with a sensitivity of 0.1 mg, and the change in weight (%) was calculated.

The pH of the PBS was also recorded at the end of each time point, and the change in pH with respect to time was plotted.

2.2.6. In vitro studies

In vitro studies were performed using L929 mouse fibroblasts (ATCC CCL-1, passage 13). Cells were suspended in DMEM containing penicillin-streptomycin (100 U/mL), and 10% FBS, and seeded on scaffolds (seeding density $= 2.4 \times 10^5$ cells/cm^3) placed in a 24-well plate. The cells were incubated for 3 weeks with refreshing of media every 3 days.

Cell proliferation on the scaffolds was studied using the alamarBlue® cell viability assay kit. Scaffolds were removed from culture at various time points (Days 1, 8 and 15), washed with PBS and incubated in 10% alamarBlue solution (in DMEM-High glucose containing 1% penicillin-streptomycin (100 U/mL)).

On Day 8, scaffolds were incubated in 4% paraformaldehyde for 15 min at room temperature, Alexa fluor 532-Phalloidin for 1 h at 37 °C, and DRAQ5 for 10 min at 37 °C. Scaffolds were examined under a confocal laser scanning microscope (CLSM) (Leica DM 2500, Germany).

Morphology of cells was studied using the CLSM images ($n = 13$–35 cells/image). For that, the shape descriptors roundness and aspect ratio were calculated using the ImageJ software.

2.2.7. Statistical analyses

Statistical analyses were performed using SPSS 23 (IBM, USA). One-way ANOVA was performed to compare the pore size, porosity, mechanical properties, weight loss, and pH. Two-way ANOVA was performed to test if there was an interaction between the independent parameters (freezing temperature and coating). Levene's test of inequality was performed to test whether samples had equal variance. Tukey's HSD (equal variance) or Dunnett's T3 (unequal variance) *post hoc* tests were performed after ANOVA. A significance level (α) of 0.05 was used. Data are presented as the mean ± standard deviation (SD).

3. Results

3.1. Scaffold microarchitecture

SEM examination revealed that scaffold microarchitecture varied considerably with the change in freezing temperature and upon alginate-coating (Fig. 1). Pore size decreased when the preparation temperature was lowered from −20 °C (Fig. 1A) to −80 °C (Fig. 1B). Alginate on the surface of the scaffolds was very thin, and it slightly decreased the pore size.

Quantitative analysis of the SEM images revealed that pore size decreased with the decrease in preparation temperature ($p < 0.01$) and with alginate-coating ($p < 0.05$) (Fig. 2A). Pore size of the uncoated scaffolds was 127 ± 80 μm when prepared at −20 °C, and 65 ± 39 μm when prepared at −80 °C. That of the coated scaffolds was 112 ± 77 μm when prepared at −20 °C, and 39 ± 24 μm when prepared at −80 °C. The

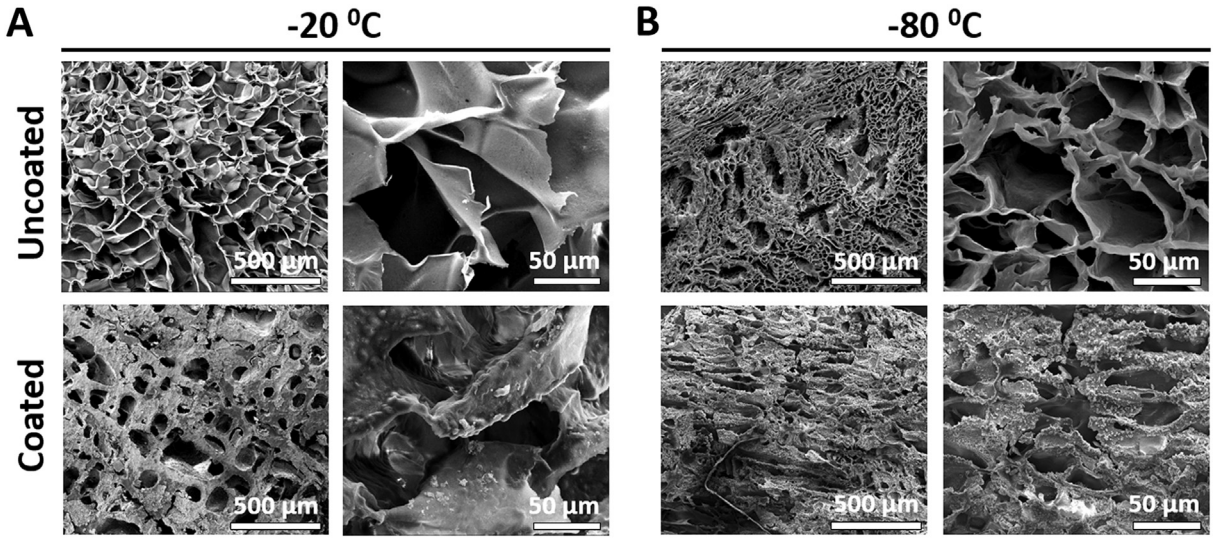

Fig. 1. SEM images showing the scaffold microarchitecture. Scaffolds prepared at (A) −20 °C, and (B) −80 °C prior to lyophilization. Upper panel: uncoated scaffolds, and lower panel: alginate-coated.

effect of temperature on pore size was more distinct than that of alginate-coating (2-way ANOVA).

Mercury porosimetry verified these results (Fig. S1). Pore size of the scaffolds prepared at −20 °C was in the range 30–200 μm, while that prepared at −80 °C was in the range 10–100 μm. Alginate-coating decreased the pore size of the scaffolds (a decrease in pore size in the range 10–50 μm).

Porosity, on the other hand, was in the range 60–65%, and did not change significantly with coating or preparation temperature (Fig. 2B).

3.2. Compressive properties of the scaffolds

Compressive testing revealed that lowering the preparation temperature resulted in significantly higher compressive modulus ($p < 0.001$) (Fig. 3A) and strength ($p < 0.001$) (Fig. 3B). Alginate-coating had no effect on the compressive properties of scaffolds. Compressive modulus of the scaffolds prepared at −20 °C was 586 ± 97 kPa when scaffolds were uncoated, and 633 ± 105 kPa when they were coated (Fig. 3A). Modulus of scaffolds prepared at −80 °C was 1497 ± 98 kPa when scaffolds were uncoated, and 1415 ± 153 kPa when they were coated. On the other hand, compressive strength of the scaffolds prepared at −20 °C was 45 ± 11 kPa when scaffolds were uncoated, and 35 ± 5 kPa when they were coated (Fig. 3B). That of scaffolds prepared at −80 °C was 110 ± 12 kPa when scaffolds were uncoated, and 128 ± 18 kPa when they were coated.

3.3. Degradation of the scaffolds

Degradation tests revealed a significant loss of weight with the alginate-coated scaffolds over time ($p < 0.05$), while no or little weight loss was observed with the uncoated scaffolds (Fig. 4A). At the end of 8-week incubation period, uncoated scaffolds lost 5% of their weight, while coated scaffolds lost 40% of their weight. The pH of the coated scaffold medium also decreased significantly over time (from 7.2 to around 6.6) ($p < 0.05$), while that of the uncoated scaffolds decreased slightly (from 7.2 to around 7.0) ($p > 0.05$) (Fig. 4B).

The dry weight and pH levels reached a plateau after Week 4, suggesting that most of the alginate was degraded by that time.

3.4. Cell proliferation

AlamarBlue cell viability assay revealed a significantly higher number of cells on the uncoated scaffolds than the coated ones on Day 15 ($p < 0.05$) (Fig. 5). This meant that the cell proliferation rate was higher on the uncoated scaffolds than that on the coated ones. Scaffold preparation temperature had no effect on cell proliferation.

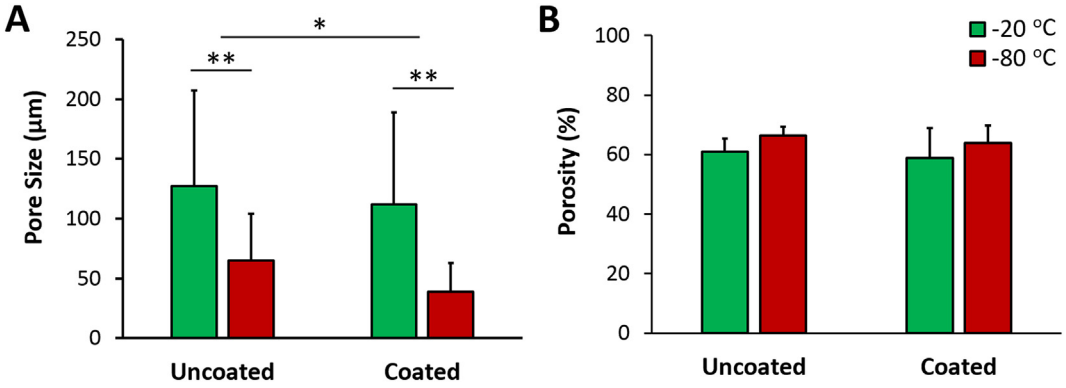

Fig. 2. Quantitative measurement of pore size and porosity of the scaffolds. (A) Pore size, and (B) porosity (%). Data are presented as the mean ± SD. Significant difference after two-way ANOVA: *$p < 0.05$, **$p < 0.01$.

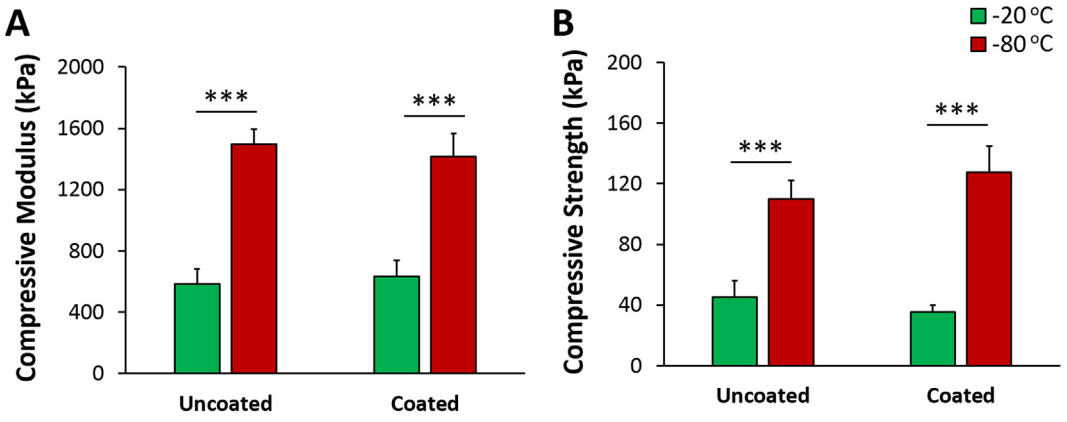

Fig. 3. Compressive mechanical properties of the scaffolds under wet conditions (after incubation in PBS for 24 h). (A) Compressive modulus, and (B) compressive strength. Data are presented as the mean ± SD. Significant difference after two-way ANOVA: ***$p < 0.001$.

3.5. Cell morphology

Morphology of the cells was examined using confocal microscopy (Fig. 6). Cells on the uncoated scaffolds prepared at −20 °C were round/elongated with few cellular extensions (lamellipodia/filopodia) after 8 days of incubation in culture media (Fig. 6A). When the scaffolds were coated, however, cells protruded more cell extensions and exhibited a more dendritic/elongated morphology.

On the uncoated scaffolds prepared at −80 °C, cells exhibited a more round morphology than those on scaffolds prepared at −20 °C, but had higher number of extensions. Similarly, coating with alginate resulted in a more dendritic/elongated morphology and longer cellular extensions.

Quantitative analysis also showed that cells tended to get more round when the scaffold preparation temperature was lower (−80 °C) (Fig. 6B). However, when coated with alginate, cells tended to get less round. Coating with alginate was more effective in determining the cell morphology than the temperature (two-way ANOVA). Cells tended to get more elongated (higher aspect ratio) with the increasing preparation temperature (−20 °C) and with coating (Fig. 6C).

4. Discussion

In order to study the effects of preparation (freezing) temperature and alginate-coating of the lyophilized scaffolds on cell behavior, PLLA/PLGA based scaffolds using two different freezing temperatures (−20 and −80 °C) were prepared, exposed to oxygen plasma and coated with alginate (coated group). As controls, a group of the scaffolds were not coated with alginate (uncoated group). First, the effects of preparation temperature and alginate-coating on porosity and pore size of the scaffolds were tested.

Porosity did not change with the change in preparation temperature or with alginate-coating. The decrease in freezing temperature (increase in cooling rate) resulted in smaller pores (Fig. 2A), due to faster formation of crystals during freezing of the solvent (1,4-dioxane), which in turn resulted in a higher number of crystals. Thus, the crystals were small, and when they were sublimed during lyophilization process, they formed smaller pores [12]. Similar observations were made in other studies; higher cooling rates resulted in smaller pores [4,5,46,47].

The smaller pores also led to higher mechanical properties. Scaffolds prepared at −80 °C exhibited significantly higher compressive modulus and strength than those prepared at −20 °C (Fig. 3). Scaffolds with smaller pores were reported to exhibit higher mechanical properties [5,46–48] as in the current study, although the shape of the pores also influenced the results.

Degradation/dissolution of the scaffolds was also monitored by measuring their dry weight every 2 weeks during the eight-week incubation period (Fig. 4A). Alginate-coated scaffolds lost 40% of their weight by Week 8, and most of this weight was lost in the first 2–4 weeks of incubation. Conversely, the uncoated scaffolds lost only 5% of their weight after 8 weeks of incubation. The reason for these different degradation profiles could be the surface chemistry. Uncoated PLLA/PLGA scaffolds resisted hydrolytic degradation, because they are hydrophobic and lack functional groups. On the other hand, the alginic acid is hydrophilic (has hydroxyl and carboxyl groups), which might enable easy access of water to, and hydrolytic degradation/dissolution of, the alginate backbone. Similar results were reported in the literature. We previously

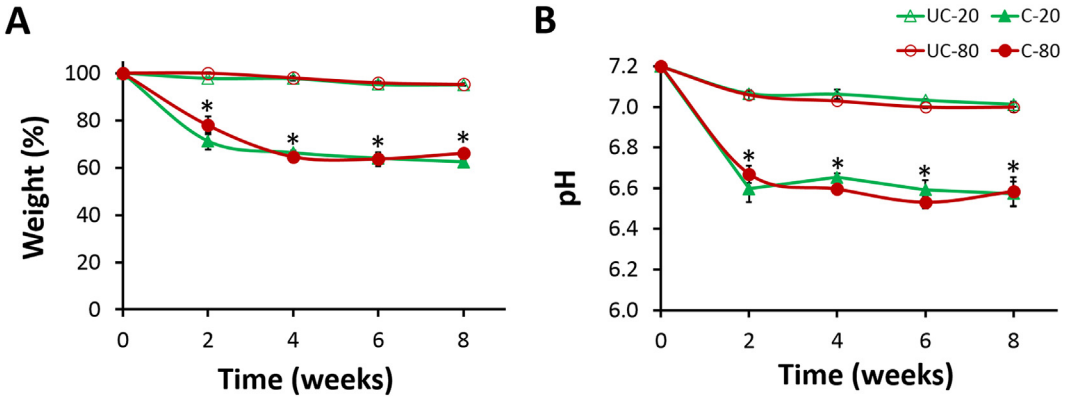

Fig. 4. Degradation profile of scaffolds incubated for 8 weeks in PBS at 37 °C. The changes in (A) dry weight and (B) pH of the scaffolds in time. Data are presented as the mean ± SD. Significant difference after two-way ANOVA: *$p < 0.05$ for the coated (C) samples compared to uncoated (UC).

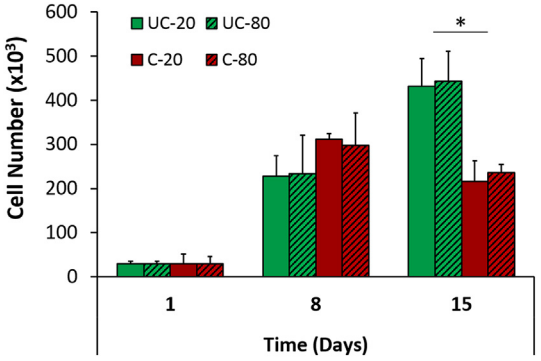

Fig. 5. Number of L929 fibroblasts on scaffolds as determined with alamarBlue assay. Data are presented as the mean ± SD. Significant difference after two-way ANOVA: *p < 0.05.

showed that the uncoated PLLA/PLGA scaffolds lost 10% of their weight after 2 weeks of incubation in culture media, while the alginate-coated scaffolds lost 40% of their weight [46]. Similarly, PLLA-based scaffolds were reported to maintain their architecture and mechanical properties 8 weeks after implantation into mice [49], while alginate hydrogels were reported to lose their mechanical properties in just 2 days *in vitro* and degrade completely only after 14 days *in vivo* in a rat model [50].

Rapid degradation/dissolution of alginate resulted in a decrease in the pH of the environment (Fig. 4B), due to release of alginic acid residues upon degradation/dissolution. This, in turn, could lead to even faster degradation of the PLLA/PLGA backbone when the scaffolds were coated, due to the autocatalytic effect [51].

Cell number was higher on the uncoated scaffolds than on the coated ones (Fig. 5). The reason for this could be the hydrophilicity of alginate, which results in absorption of water molecules preventing the cells from attaching on the scaffolds. In addition, alginate does not have bioactive sites which help in cell adhesion [52]. Moreover, alginate is soft and could lead to weak cell adhesion and proliferation. In line with our finding, fibroblasts were reported to have lower cell numbers on the alginate-coated PLLA/PLGA scaffolds than the uncoated ones [46]. Recently, we reported that proliferation rate of the fibroblasts increased with the increasing stiffness [5]. Other researchers reported no effect of stiffness on the proliferation rate of the fibroblasts [25]. However, they used polyacrylamide gels with a stiffness range 0.3–55 kPa, which may be the reason for the different results they reported. Another reason for the lower cell number on the alginate-coated scaffolds could be the rapid degradation/dissolution of alginate, which probably resulted in loss of material and cells on the surface of the scaffolds.

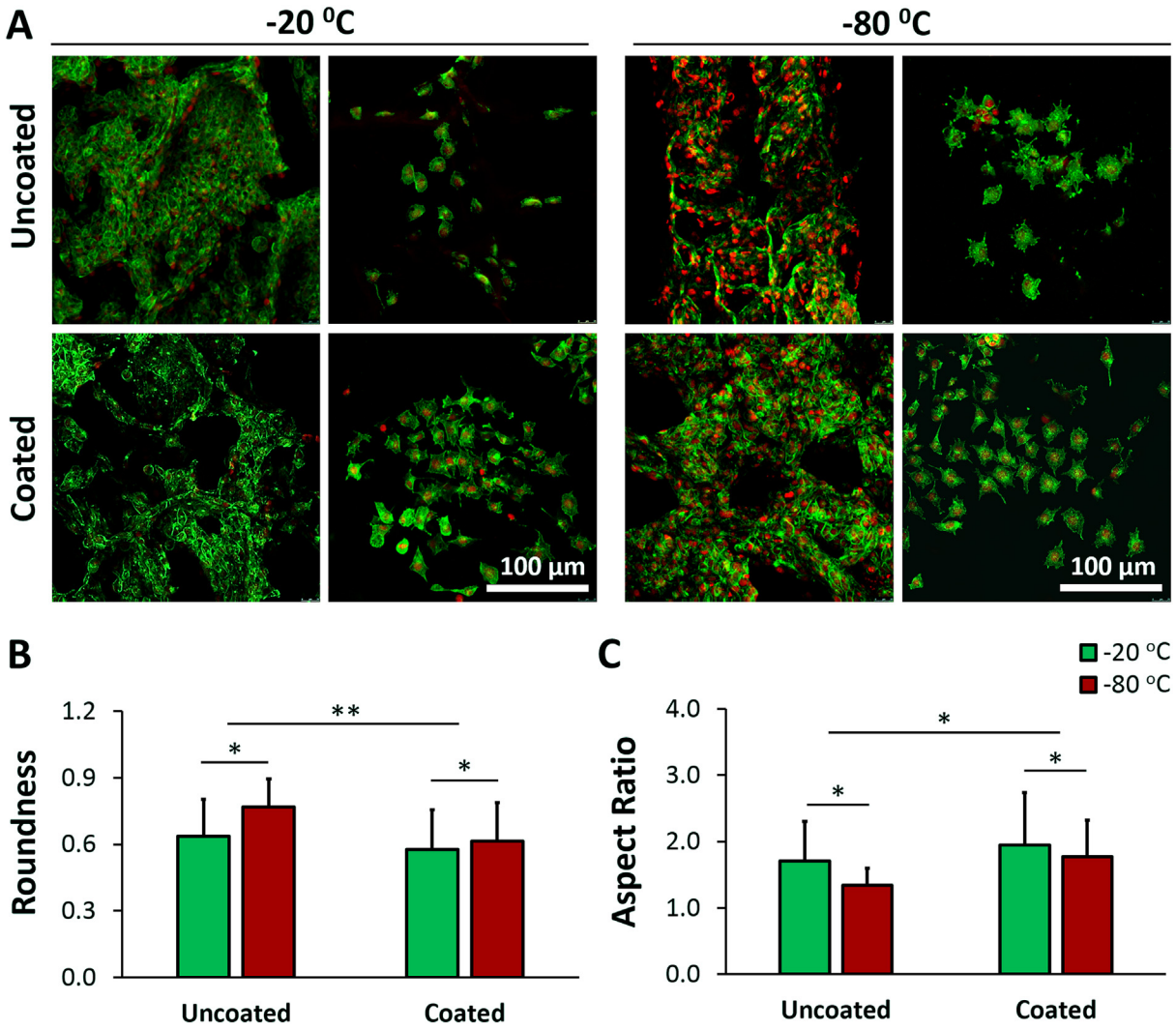

Fig. 6. Morphology of the L929 fibroblasts on scaffolds after 8 days of incubation. (A) Confocal laser scanning microscopy (CLSM) images of the cell-seeded scaffolds prepared at −20 °C (left) or −80 °C (right) prior to lyophilization. Upper panel: uncoated, and lower panel: alginate-coated. Nuclei were stained with DRAQ5 (red), and cytoskeleton with Alexa fluor 532-phalloidin (green). Morphology of the cells was analyzed quantitatively with ImageJ using the shape descriptors, (B) roundness and (C) aspect ratio. Data are presented as the mean ± SD. Significant difference after two-way ANOVA: *p < 0.05, **p < 0.01.

Rapid degradation/dissolution of alginate probably resulted in rapid drop in the pH of the medium, which might affect the cell viability. Sung and colleagues [53] reported that *in vitro* cell viability was lower on the degradable scaffolds when the degradation rate was higher; PLA scaffolds (degradation rate: high) exhibited lower cell viability than the PCL scaffolds (degradation rate: low). They also showed that PLA-based scaffolds exhibited less cell attachment (immobilization) and angiogenesis after subcutaneous implantation into mice. These were explained with the acidic environment created by the release of the degradation byproducts, which affected the cells negatively. These finding are similar to our results.

Pore size had no effect on cell proliferation, since no difference was observed between scaffolds prepared at −20 °C and those prepared at −80 °C (Fig. 5). In our previous study, we also showed that pore size had no effect on cell proliferation rate of the fibroblasts [5]. Some researchers reported optimal pore size for cell proliferation [12,17], while others reported increased cell proliferation rate with the decreasing pore size [4].

Cell morphology changed with the scaffold preparation temperature and coating (Fig. 6). Cells tended to get more round (high roundness and low aspect ratio values) at the lower preparation temperature (−80 °C), and more dendritic/elongated (low roundness and high aspect ratio values) upon coating with alginate. Two-way ANOVA revealed that alginate-coating is more effective in determining the cell morphology. Lowering the preparation temperature resulted in smaller pores and stiffer scaffolds, while alginate-coating resulted in smaller pores but had no effect on stiffness of the scaffolds, although the surface of the scaffold would be softer than the uncoated PLLA/PLGA scaffolds (Figs. 2 and 3). Two-way ANOVA also revealed that the preparation temperature was more effective in determining the pore size than coating with alginate. Considering all these, one can deduce that cell morphology is dependent on the stiffness and pore size. Cells get more round with the increasing stiffness and decreasing pore size. Cells are known to have a more branched morphology on the scaffolds with stiffness matching their own stiffness [40]. When the stiffness of a scaffold gets closer to that of the fibroblasts, the cells assume more branched morphology. In parallel to our study, fibroblasts were reported to exhibit more branched morphology on the softer scaffolds [5,13,29].

However, since alginate-coating had more effect on cell morphology than the preparation temperature (Fig. 6B and C), there might be other reasons affecting the cell morphology when alginate was introduced. One reason might be the hydrophilicity of alginate. It seems that changing the hydrophobic surface of the PLLA/PLGA scaffold to hydrophilic (by coating it with alginate) results in more dendritic/elongated morphology. In fact, cell attachment has been reported to be optimal on the slightly hydrophilic surfaces (contact angle of around 65°) rather than the hydrophobic ones [53,54]. Another reason could be the softness of alginate. Although alginate did not affect the overall mechanical properties of the scaffolds, it provided a soft environment for the cells on the surface of the scaffolds (stiffness of alginate: 4 kPa) [44] that matched the stiffness of the fibroblasts (again 4 kPa) [41]. This could explain the more branched cell morphology on the alginate coated scaffolds.

When the preparation temperature increased, cells assumed more branched/elongated morphology on the alginate-coated scaffolds (Fig. 6). The most branched cell morphology was obtained when the scaffolds were prepared at −20 °C and coated with alginate. This shows that fibroblasts sensed the modulus of the PLLA/PLGA scaffold even after coating it with alginate.

In summary, presence of alginate-coating resulted in decreased pore size, decreased pH and increased degradation/dissolution rate of the scaffolds. Alginate also led cells to elongate and protrude more cell extensions. The decreasing preparation temperature resulted in decreased pore size and increased compressive properties, which in turn, could be the reasons for the round cell morphology and increased number of cell extensions.

5. Conclusions

In this study, the effects of preparation temperature and alginate-coating of the lyophilized PLLA/PLGA scaffolds on cell behavior were investigated. Cell proliferation rate was shown to decrease with alginate-coating, but not to change with the preparation temperature. Cell proliferation rate was low on the alginate-coated scaffolds, probably because of (i) the rapid degradation/dissolution of alginate, which results in loss of material and cells, (ii) rapid drop in pH of the environment, which limits cell viability, (iii) softness of alginate which leads to low cell proliferation rate, and (iv) hydrophilicity of alginate, which results in water absorption around the scaffolds and limits cell adhesion. Cells were also shown to get more branched in the presence of alginate and with the increasing preparation temperature of the scaffolds. The branched cell morphology was probably related to (i) the small pore size, which provided more contact area for the cells to protrude their lamellipodia/filopodia, (ii) softening of the bulk (by increasing the preparation temperature) and surface (by coating with alginate) stiffness. This study is significant in that it shows that cells could be directed to have different phenotypes by changing the surface stiffness and hydrophilicity of the scaffolds without changing their bulk stiffness. Thus, tissues of different biochemical properties could be engineered using the same cells. In fact, the spatial heterogeneity of the native tissues could be recapitulated by locally modifying the scaffolds and altering the cell behavior on these regions. This shows the importance of material stiffness, surface chemistry, and cell-material interactions in designing engineered tissues. Our future studies will include the analysis of the effect of stiffness and alginate-coating on cell differentiation and ECM production, and the test of our scaffolds *in vivo*.

Supplementary data to this article can be found online at https://doi.org/10.1016/j.ijbiomac.2018.11.169.

Acknowledgements

This project was supported by BIOMATEN, Middle East Technical University [grant number: BAP-08-11-2016-022] and Ministry of Industry and Commerce of Turkey [grant number: SanTez 00356.STZ.2009-1]. GB was supported by TUBITAK [through Bideb 2214/A].

Competing interest statement

The authors declare that there is no conflict of interests.

Author contributions

GB: collection and analysis of data, and preparation of manuscript.

GB, NH and VH: study design, interpretation of data, and revision of manuscript.

VH and NH: supervision of the project, funding.

References

[1] R. Langer, J.P. Vacanti, Tissue engineering, Science 260 (1993) 920–926.
[2] M.A. Sweigart, K.A. Athanasiou, Toward tissue engineering of the knee meniscus, Tissue Eng. 7 (2001) 111–129.
[3] C.J. Koh, A. Atala, Therapeutic cloning and tissue engineering, Curr. Top. Dev. Biol. 60 (2004) 1–15.
[4] B.B. Mandal, S.C. Kundu, Cell proliferation and migration in silk fibroin 3D scaffolds, Biomaterials 30 (2009) 2956–2965.
[5] G. Bahcecioglu, N. Hasirci, V. Hasirci, Effects of microarchitecture and mechanical properties of 3D microporous PLLA-PLGA scaffolds on fibrochondrocyte and L929 fibroblast behavior, Biomed. Mater. 13 (2018), 035005.
[6] A.G. Mikos, M.D. Lyman, L.E. Freed, R. Langer, Wetting of poly(L-lactic acid) and poly (DL-lactic-coglycolic acid) foams for tissue culture, Biomaterials 15 (1994) 55–58.
[7] B.S. Kim, D.J. Mooney, Development of biocompatible synthetic extracellular matrices for tissue engineering, Trends Biotechnol. 16 (1998) 224–230.
[8] D.W. Hutmacher, Scaffolds in tissue engineering bone and cartilage, Biomaterials 21 (2000) 2529–2543.
[9] M.A. Schwartz, C.S. Chen, Deconstructing dimensionality, Science 339 (2013) 402–404.
[10] P. Friedl, K. Wolf, Plasticity of cell migration: a multiscale tuning model, J. Cell Biol. 188 (2010) 11–19.

[11] L.G. Griffith, Emerging design principles in biomaterials and scaffold for tissue engineering, Ann. N. Y. Acad. Sci. 961 (2002) 83–95.
[12] F.J. O'Brien, B.A. Harley, I.V. Yannas, L.J. Gibson, The effect of pore size on cell adhesion in collagen-GAG scaffolds, Biomaterials 26 (2005) 433–441.
[13] M. Miron-Mendoza, J. Seemann, F. Grinnell, The differential regulation of cell motile activity through matrix stiffness and porosity in three dimensional collagen matrices, Biomaterials 31 (2010) 6425–6435.
[14] J. Klompmaker, H.W. Jansen, R.H. Veth, H.K. Nielsen, J.H. de Groot, A.J. Pennings, Porous implants for knee joint meniscus reconstruction: a preliminary study on the role of pore sizes in ingrowth and differentiation of fibrocartilage, Clin. Mater. 14 (1993) 1–11.
[15] A.K. Salem, R. Stevens, R.G. Pearson, M.C. Davies, S.J.B. Tendler, C.J. Roberts, P.M. Williams, K.M. Shakesheff, Interactions of 3T3 fibroblasts and endothelial cells with defined pore features, J. Biomed. Mater. Res. 61 (2002) 212–217.
[16] J. Yang, G. Shi, J. Bei, S. Wang, Y. Cao, Q. Shang, G. Yang, W. Wang, Fabrication and surface modification of macroporous poly(L-lactic acid) and poly(L-lactic co-glycolic acid) (70/30) cell scaffolds for human skin fibroblasts cell culture, J. Biomed. Mater. Res. 62 (2002) 438–446.
[17] C.M. Murphy, M.G. Haugh, F.J. O'Brien, The effect of mean pore size on cell attachment, proliferation and migration in collagen–glycosaminoglycan scaffolds for bone tissue engineering, Biomaterials 31 (2010) 461–466.
[18] C.M. Murphy, G.P. Duffy, A. Schindeler, F.J. O'Brien, Effect of collagen-glycosaminoglycan scaffold pore size on matrix mineralization and cellular behavior in different cell types, J. Biomed. Mater. Res. A 104 (2016) 291–304.
[19] W.K. Grier, E.M. Iyoha, B.A. Harley, The influence of pore size and stiffness on tenocyte bioactivity and transcriptomic stability in collagen-GAG scaffolds, J. Mech. Behav. Biomed. Mater. 65 (2017) 295–305.
[20] B.A. Harley, H.D. Kim, M.H. Zaman, I.V. Yannas, D.A. Lauffenburger, L.J. Gibson, Microarchitecture of three-dimensional scaffolds influences cell migration behavior via junction interactions, Biophys. J. 95 (2008) 4013–4024.
[21] E. Tamjid, A. Simchi, J.W. Dunlop, P. Fratzl, R. Bagheri, M. Vossoughi, Tissue growth into three-dimensional composite scaffolds with controlled micro-features and nanotopographical surfaces, J. Biomed. Mater. Res. A 101 (2013) 2796–2807.
[22] C.M. Lo, H.B. Wang, M. Dembo, Y.L. Wang, Cell movement is guided by the rigidity of the substrate, Biophys. J. 79 (2000) 144–152.
[23] T. Yeung, P.C. Georges, L.A. Flanagan, B. Marg, M. Ortiz, M. Funaki, N. Zahir, W. Ming, V. Weaver, P.A. Janmey, Effects of substrate stiffness on cell morphology, cytoskeletal structure, and adhesion, Cell Motil. Cytoskeleton 60 (2005) 24–34.
[24] A.J. Engler, S. Sen, H.L. Sweeney, D.E. Discher, Matrix elasticity directs stem cell lineage specification, Cell 126 (2006) 677–689.
[25] J.D. Mih, A.S. Sharif, F. Liu, A. Marinkovic, M.M. Symer, D.J. Tschumperlin, A multiwell platform for studying stiffness-dependent cell biology, PLoS One 6 (2011), e19929.
[26] M. Ehrbar, A. Sala, P. Lienemann, A. Ranga, K. Mosiewicz, A. Bittermann, S.C. Rizzi, F.E. Weber, M.P. Lutolf, Elucidating the role of matrix stiffness in 3D cell migration and remodeling, Biophys. J. 100 (2011) 284–293.
[27] B.N. Mason, A. Starchenko, R.M. Williams, L.J. Bonassar, C.A. Reinhart-King, Tuning three-dimensional collagen matrix stiffness independently of collagen concentration modulates endothelial cell behavior, Acta Biomater. 9 (2013) 4635–4644.
[28] H.Y. Mi, X. Jing, M.R. Salick, T.M. Cordie, X.F. Peng, L.S. Turng, Properties and fibroblast cellular response of soft and hard thermoplastic polyurethane electrospun nanofibrous scaffolds, J Biomed Mater Res B Appl Biomater 103 (2015) 960–970.
[29] C. Branco da Cunha, D.D. Klumpers, W.A. Li, S.T. Koshy, J.C. Weaver, O. Chaudhuri, P.L. Granja, D.J. Mooney, Influence of the stiffness of three-dimensional alginate/collagen-I interpenetrating networks on fibroblast biology, Biomaterials 35 (2014) 8927–8936.
[30] Pelham R.J. Jr., Y. Wang, Cell locomotion and focal adhesions are regulated by substrate flexibility, Proc. Natl. Acad. Sci. U. S. A. 94 (1997) 13661–13665.
[31] P.C. Georges, W.J. Miller, D.F. Meaney, E.S. Sawyer, P.A. Janmey, Matrices with compliance comparable to that of brain tissue select neuronal over glial growth in mixed cortical cultures, Biophys. J. 90 (2006) 3012–3018.
[32] A.P. Balgude, X. Yu, A. Szymanski, R.V. Bellamkonda, Agarose gel stiffness determines rate of DRG neurite extension in 3D cultures, Biomaterials 22 (2001) 1077–1084.
[33] L.A. Flanagan, Y.E. Ju, B. Marg, M. Osterfield, P.A. Janmey, Neurite branching on deformable substrates, Neuroreport 13 (2002) 2411–2415.
[34] R. Olivares-Navarrete, E.M. Lee, K. Smith, S.L. Hyzy, M. Doroudi, J.K. Williams, K. Gall, B.D. Boyan, Z. Schwartz, Substrate stiffness controls osteoblastic and chondrocytic differentiation of mesenchymal stem cells without exogenous stimuli, PLoS One 12 (2017), e0170312.
[35] M.R. Ng, A. Besser, G. Danuser, J.S. Brugge, Substrate stiffness regulates cadherin-dependent collective migration through myosin-II contractility, J. Cell Biol. 199 (2012) 545–563.
[36] Y. Arima, H. Iwata, Effect of wettability and surface functional groups on protein adsorption and cell adhesion using well-defined mixed self-assembled monolayers, Biomaterials 28 (2007) 3074–3082.
[37] H.-I. Chang, Y. Wang, Cell responses to surface and architecture of tissue engineering scaffolds, in: D. Eberli (Ed.), Regenerative Medicine and Tissue Engineering - Cells and Biomaterials, Intech Open, Rijeka, Croatia 2011, pp. 569–588.
[38] A.D. Doyle, R.J. Petrie, M.L. Kutys, K.M. Yamada, Dimensions in cell migration, Curr. Opin. Cell Biol. 25 (2013) 642–649.
[39] B. Trappmann, C.S. Chen, How cells sense extracellular matrix stiffness: a material's perspective, Curr. Opin. Biotechnol. 24 (2013) 948–953.
[40] Y. Ni, M.Y.M. Chiang, Cell morphology and migration linked to substrate rigidity, Soft Matter 3 (2007) 1285–1292.
[41] H.W. Wu, T. Kuhn, V.T. Moy, Mechanical properties of L929 cells measured by atomic force microscopy: effects of anticytoskeletal drugs and membrane crosslinking, Scanning 20 (1998) 389–397.
[42] J. Sanchez-Adams, R.E. Wilusz, F. Guilak, Atomic force microscopy reveals regional variations in the micromechanical properties of the pericellular and extracellular matrices of the meniscus, J. Orthop. Res. 31 (2013) 1218–1225.
[43] G. Sriram, P.L. Bigliardi, M. Bigliardi-Qi, Fibroblast heterogeneity and its implications for engineering organotypic skin models in vitro, Eur. J. Cell Biol. 94 (2015) 483–512.
[44] A.C. Daly, S.E. Critchley, E.M. Rencsok, D.J. Kelly, A comparison of different bioinks for 3D bioprinting of fibrocartilage and hyaline cartilage, Biofabrication 8 (2016), 045002.
[45] J.C. Park, B.J. Park, D.H. Lee, H. Suh, D.G. Kim, O.H. Kwon, Evaluation of the cytotoxicity of polyetherurethane (PU) film containing zinc diethyldithiocarbamate (ZDEC) on various cell lines, Yonsei Med. J. 43 (2002) 518–526.
[46] G. Bahcecioglu, A. Buyuksungur, A. Kiziltay, N. Hasirci, V. Hasirci, Construction and in vitro testing of a multilayered, tissue-engineered meniscus, J. Bioact. Compat. Polym. 29 (2014) 235–253.
[47] A.N. Halili, N. Hasirci, V. Hasirci, A multilayer tissue engineered meniscus substitute, J. Mater. Sci. Mater. Med. 25 (2014) 1195–1209.
[48] C. Tu, Q. Chai, J. Jang, Y. Wan, J. Bei, S. Wang, The fabrication and characterization of poly(lactic acid) scaffolds for tissue engineering by improved solid-liquid phase separation, Polym. Adv. Technol. 14 (2003) 565–573.
[49] E. Saito, E.E. Liao, W.W. Hu, P.H. Krebsbach, S.J. Hollister, Effects of designed PLLA and 50:50 PLGA scaffold architectures on bone formation in vivo, J. Tissue Eng. Regen. Med. 7 (2013) 99–111.
[50] D. Shahriari, J. Koffler, D.A. Lynam, M.H. Tuszynski, J.S. Sakamoto, Characterizing the degradation of alginate hydrogel for use in multilumen scaffolds for spinal cord repair, J. Biomed. Mater. Res. A 104 (2016) 611–619.
[51] H. Tsuji, M. Ogiwara, S.K. Saha, T. Sakaki, Enzymatic, alkaline, and autocatalytic degradation of poly(L-lactic acid): effects of biaxial orientation, Biomacromolecules 7 (2006) 380–387.
[52] G. Bahcecioglu, N. Hasirci, B. Bilgen, V. Hasirci, Hydrogels of agarose, and methacrylated gelatin and hyaluronic acid are more supportive for in vitro meniscus regeneration than 3D printed PCL scaffolds, Int. J. Biol. Macromol. (2018) https://doi.org/10.1016/j.ijbiomac.2018.09.065.
[53] H.J. Sung, C. Meredith, C. Johnson, Z.S. Galis, The effect of scaffold degradation rate on three-dimensional cell growth and angiogenesis, Biomaterials 25 (26) (2004) 5735–5742.
[54] D.P. Dowling, I.S. Miller, M. Ardhaoui, W.M. Gallagher, Effect of surface wettability and topography on the adhesion of osteosarcoma cells on plasma-modified polystyrene, J. Biomater. Appl. 6 (2011) 327–347.